RESEARCH ARTICLE

Assessment of circulating extracellular vesicles from calorie-restricted mice and humans in ischaemic injury models

Manuel S. V. Jaimes[1] | **Chia-Te Liao[2,3,4]** | **Max M. Chen[1]** | **Andreas Czosseck[1]** | **Tsung-Lin Lee[2]** | **Yu-Hsiang Chou[5]** | **Yung-Ming Chen[5]** | **Shuei-Liong Lin[5,6]** | **James J. Lai[7,8]** | **David J. Lundy[1,9,10]** (iD)

[1]Graduate Institute of Biomedical Materials & Tissue Engineering, Taipei Medical University, Taipei, Taiwan

[2]Division of Nephrology, Department of Internal Medicine, Shuang Ho Hospital, Taipei Medical University, New Taipei, Taiwan

[3]Division of Nephrology, Department of Internal Medicine, School of Medicine, College of Medicine, Taipei Medical University, Taipei, Taiwan

[4]TMU Research Center of Urology and Kidney (TMU-RCUK), Taipei Medical University, Taipei, Taiwan

[5]Division of Nephrology, Department of Internal Medicine, National Taiwan University Hospital, College of Medicine, National Taiwan University, Taipei, Taiwan

[6]Graduate Institute of Physiology, College of Medicine, National Taiwan University, Taipei, Taiwan

[7]Department of Bioengineering, University of Washington, Seattle, Washington, USA

[8]Department of Materials Science and Engineering, National Taiwan University of Science and Technology, Taipei, Taiwan

[9]International PhD Program in Biomedical Engineering, Taipei Medical University, Taipei, Taiwan

[10]Center for Cell Therapy, Taipei Medical University Hospital, Taipei, Taiwan

Correspondence
David J. Lundy, Graduate Institute of Biomedical Materials & Tissue Engineering, Taipei Medical University, Taipei, Taiwan
Email: dlundy@tmu.edu.tw

Abstract
Calorie restriction (CR) and fasting affect lifespan, disease susceptibility and response to acute injury across multiple animal models, including ischaemic injuries such as myocardial infarction or kidney hypoxia. The cargo and function of circulating extracellular vesicles (EV) respond to changes in host physiology, including exercise, injury, and other interventions. Thus, we hypothesised that EVs induced following CR may reflect some of the beneficial properties of CR itself. In a pilot study, EVs were isolated from mice following 21 days of 30 % CR, and from eight human donors after 72 h water-only fasting. EV size, concentration and morphology were profiled by NTA, western blot and cryoEM, and their function was assessed using multiple assays related to ischaemic diseases. We found that EVs from post-fasting samples better protected cardiac cells from hypoxia/reperfusion (H/R) injury compared to pre-fasting EVs. However, there was no difference when used to treat H/R-injured kidney epithelial cells. Post-fasting derived EVs slowed the rate of fibroblast migration and slightly reduced macrophage inflammatory gene expression compared to pre-fasting derived EVs. Lastly, we compared miRNA cargos of pre- and post-fasting human serum EVs and found significant changes in a small number of miRNAs. We conclude that fasting appears to influence EV cargo and function, with varied effects worthy of further exploration.

- -

1 | INTRODUCTION

1.1 | Ischaemic diseases

Ischaemic diseases are the most frequent causes of death in the world, causing more global deaths than all cancers combined (World Health Organization). Hypoxia renders cells unable to produce sufficient ATP, resulting in mitochondrial damage, apoptosis and/or necrosis of parenchymal cells, and eventual loss of functional tissue (Ojha et al., 2008; Scarabelli et al., 2001). Heart (myocardial infarction), brain (thrombotic stroke), kidney (renal ischaemia) and skeletal muscle (critical limb ischaemia) are the most common sites of hypoxic injury. In the clinic, the gold standard of care is the rapid restoration of blood flow, aiming to prevent additional cell death, minimise infarct volume and preserve organ function. However, reperfusion also induces a second wave of injury, caused by rapid pH change, reactive oxygen species (ROS) generation and calcium overload (Prasad et al., 2009). Upon ischaemia/reperfusion injury, it has been shown that macrophages play a crucial role in regulating tissue damage and repair, depending on their phenotypic/functional states (or polarisation) (Shin et al., 2022). Macrophage polarisation can be roughly categorised into M1 ("pro-inflammatory") and M2 ("anti-inflammatory or reparative") polarisation (Murray et al., 2014). Although simplistic, this classification has been widely utilised to understand the role of macrophages within specific disease scenarios. For therapy of ischaemia many strategies have been explored to provide small molecules, growth factors, cytokines or miRNAs which can buffer against parenchymal cell death, and/or modulate local the immune response, particularly macrophage polarisation, at the time of reperfusion (Gerczuk & Kloner, 2012).

1.2 | Extracellular vesicles

Body fluids are rich in micro- and nano-scale particles secreted from cells. These particles include phospholipid bilayer membrane-bound extracellular vesicles (EVs), comprising apoptotic bodies, microvesicles and exosomes (Théry et al., 2018). The smallest population includes exosomes (~100 nm diameter), which are secreted by exocytosis. EVs carry payloads of proteins (including growth factors, cytokines) and genetic material (mRNA, miRNAs, lncRNAs) which have powerful, combinatorial biologic effects (Barile et al., 2017; George et al., 2022; Kugeratski et al., 2021). Proteomic analysis has found approximately 1200 proteins present in EVs isolated from a variety of sources, with only 22 being universally enriched. This illustrates the considerable diversity in the EV cargo, which depends on the originating cell types (Kugeratski et al., 2021) There is further variation between EV subpopulations which possess distinct RNA profiles and proteomes, which in turn have differential effects on recipient cells (Willms et al., 2016). Critically, EV quantity, content and bioactivity reflects the nature/condition of the cells which produced them. For example, many stem cells secrete EVs bearing pro-regenerative, anti-inflammatory cargo which can show tissue-protective effects (Barile et al., 2014; Czosseck et al., 2022; Gallet et al., 2017). However, EVs derived from the plasma of patients with dilated cardiomyopathy were able to transfer the same pathogenic phenotype to healthy cultured cardiomyocytes (Shah et al., 2018).

1.3 | Calorie restriction

Controlled studies using animal models of calorie restriction (CR) have shown improved survival in some cancers, delayed neurodegeneration, improved cognitive function (problem solving, memory), improved physical performance (balance, endurance, strength) and many other beneficial effects (Nencioni et al., 2018). It is also well-described that CR dramatically extends the "health-span" (time to disease onset) and lifespan of more than 20 species ranging from yeast and nematode worms to rodents, canines and non-human primates, in both healthy and disease-model animals (Colman et al., 2009). The underlying mechanisms are complex and diverse, including increased rates of DNA repair, enhanced autophagy, improved clearance of misfolded proteins, mitochondrial fusion and metabolic efficiency, immunomodulation towards a less chronic inflammatory state, alterations in mTOR activation, reduced IGF-1 levels, and many others (Most et al., 2017).

Calorie restriction has also been explored in the context of acute disease models. With regards to ischaemic disease, robust experiments in mice found that lifelong CR prior to myocardial ischaemia/reperfusion surgery significantly reduced cardiac injury and preserved cardiac function (Edwards et al., 2010). A similar study showed that a short-term 30 % reduction in calorie intake protected mice from renal ischaemia injury (Mitchell et al., 2010). Importantly, this study showed that protection could be induced by only 2–4 weeks CR in otherwise *ad libitum*-fed mice. However, it was not known whether these are local

adaptations at the tissue level, or systemic changes brought about through paracrine effects. Supporting the latter hypothesis, a 2020 study published in *Science* found that plasma from exercised animals could be transplanted into non-exercised animals, transferring neurological benefits to the sedentary animals (Horowitz et al., 2020). The authors identified the bioactive factor as glycosylphosphatidylinositol (GPI)–specific phospholipase D1 (Gpld1) which was secreted by the liver into circulation in response to exercise. Regarding circulating EVs specifically, a 2021 study also found that both resistance training and aerobic exercise altered EV cargo in human blood plasma (Vanderboom et al., 2021). EVs derived from mouse hearts after MI induction promoted pro-inflammatory behaviour, influenced macrophage polarisation, and aggravated heart injury in recipient mice (Ge et al., 2021). In another study, one night of sleep deprivation (in mice) altered circulating EVs to have more pro-thrombotic effects (Wang et al., 2022). Exercise has been shown (in mice) promote mobilisation of EVs from brown adipose tissue which contained cardioprotective miRNAs (Zhao et al., 2022). Recently, ischaemic preconditioning (in rats) altered circulating EVs towards a more cardioprotective phenotype (Luo et al., 2023). Taken together, it is clear that the physiological state of the donor steers EV cargos towards beneficial or deleterious phenotypes. Since CR appears to induce an anti-inflammatory, pro-reparative, pro-regenerative physiological state, we hypothesised that circulating EVs derived from calorie-restricted subjects would tend towards this same phenotype. These EVs could therefore have beneficial effects on recipient cells.

Since immune function naturally declines with age, the links between CR, ageing and immune function have been widely investigated. Data from lab animals are mixed but studies have shown that young and aged mice form weaker immune responses to influenza infection following CR (Gardner, 2005; Ritz et al., 2007). CR mice have also been shown to be more vulnerable to parasitic infections (Kristan, 2007). Calorie restricted C57BL/6 mice were also more susceptible to death following sepsis than their *ad libitum*-fed counterparts (Sun et al., 2001). Interestingly, peritoneal macrophages isolated from the CR mice were less responsive to lipopolysaccharide (LPS) stimulation than their well-fed counterparts. Lastly, Vega and colleagues showed C57BL/6 mouse macrophages had altered responses to LPS in accordance with CR and mouse age (Vega et al., 2004). Thus, there are clear links between CR/fasting, immune function and macrophage activity and we hypothesised that EVs derived after CR may have immunosuppressive functions.

There are some limitations of CR/fasting for use as a therapy. With the exception of scheduled surgeries, it is not possible to accurately predict when an injury will occur so that the patient can initiate CR beforehand. Secondly, outside of the lab environment, patient compliance with dietary restriction has shown to be very poor in most settings. For example, in a recent study using 4-day calorie restriction (200–1000 kcal/day) as an adjuvant therapy for breast cancer, only 33.8 % of patients successfully completed the full course of the planned calorie restriction (de Groot et al., 2020). Thus, if purified EVs from fasted subjects, or their key components (i.e., particular miRNAs or peptides) could offer therapeutic effects without the need for dietary restrictions, this could be of clinical benefit.

Based on the aforementioned evidence, we hypothesised that CR would affect the function and cargo of circulating EVs. Since most of the published literature is in mice, we first carried out a controlled pilot study in mice using a standard model of CR. However, we primarily sought to focus on human subjects since this is more relevant to human health and disease. To screen for differences in EV function we assessed the effects of pre-/post-fasting EVs in models of cardiomyocyte hypoxia, kidney hypoxia, fibroblast wound healing/migration, and macrophage polarisation. Lastly, we aimed to carry out preliminary comparisons of EV miRNA cargo from human donors before and after fasting.

2 | METHODS

2.1 | Animal calorie restriction

Mouse experiments were carried out with ethical approval by the Institutional Care and Use of Animals Committee, Taipei Medical University (protocol LAC-2021-0109) and Academia Sinica (protocol 17-11-1117). Male C57BL/6J mice were purchased from Lasco, Taiwan. These are a widely-studied rodent model for CR, known to suitably mimic human processes (Mahoney et al., 2006). Mice were 8 weeks old at the beginning of the experiment. Animals were housed in individual cages within the animal facility of Academia Sinica, Taiwan, with a 12/12 light/dark cycle. For the first 28 days, all mice were provided with food on an *ad libitum* basis to acclimatise them to the lab environment and establish their baseline energy intake. To minimise the effects of circadian variation, mice were weighed at 9:30 am every Tuesday morning and their food consumption was measured by weighing the food every Tuesday and Friday at 9:45 am. A standard lab diet of PicoLab Rodent Diet 20 was provided. This chow provides gross energy of 4.07 kcal/gram, with 24.65 % of energy coming from protein, 13.21 % from fat and 62.14 % from carbohydrates. Calorie reduction of 30 % has been previously shown to improve health and lifespan of C56BL/6J mice (Mitchell et al., 2019). Therefore, mice in the calorie restriction (CR) group were subjected to a 30 % reduction in calorie intake by means of weighing and providing exact amounts of dry food pellets in accordance with body weight. At 16:00 on the final day of calorie restriction (day 20), all food was removed from the cages until 09:30 the next morning. Water was provided *ad libitum* at all times. A group of 10 control mice, from the same batch of the same supplier, housed at the same facility, were provided an *ab libitum* diet for the whole experimental duration. To collect blood, animals were anaesthetised by inhaled isoflurane and

blood was slowly collected by cardiac puncture using a 24 g needle into EDTA-coated paediatric blood collection tubes (BD), then centrifuged at 2000 g for 10 min at 4°C. Plasma was aliquoted and frozen at −80°C for further analysis, which was within 2 weeks of sampling. This protocol follows best practice guidelines from the International Society of Extracellular Vesicles (ISEV) (Théry et al., 2018; Witwer et al., 2013). EVs were then extracted using a validated commercial kit, ExoPure (BioVision, K1238-2). The manufacturer protocol was followed precisely.

2.2 | Human calorie restriction

Human experiments were approved by the Institutional Review Board (IRB) at Taipei Medical University, under protocol number N202104120. We sought to recruit male and female subjects, aged between 21 and 65, body weight of ≥50 kg, BMI ≥ 18 ≤ 30. Exclusion criteria included type I or II diabetes, diagnosed cardiovascular disease, hypertension, hypotension, pregnancy or anaemia. Subjects fasted from the night prior until the first blood sample (12 h) to reduce the presence of circulating products of digestion in the samples. Subjects then consumed only water for an additional 72–96 h. Thus, the total period of fasting was 84–108 h. Informed consent was obtained from all subjects, and the experimental aims and hypothesis were explained in full. Subjects were provided with a written document and orally counselled regarding potential adverse events, including psychological, social and physiological effects. Subjects were contacted at least once per day to monitor compliance and welfare, and were instructed to follow their normal daily routines, including continuation of any routine medication. Subjects were instructed to consume only water (calorie-free food and other beverages were explicitly forbidden) for the study period, and all subjects self-reported compliance. Beta hydroxybutyrate (BHB) ketone levels in serum were measured, by the study researchers, using a calibrated test device (eBKetoLife, Visgeneer). Body weight was recorded in the morning, thus standardising for circadian rhythm. Venous blood samples were collected into serum separation tubes, gently mixed, and allowed to coagulate at room temperature for 30 min. Tubes were centrifuged at 2500 g for 15 min at 4 °C and extracellular vesicles were isolated using the ExoQuick LP (AMS Bio) system, precisely following the manufacturer protocol.

2.3 | Nanoparticle Tracking Analysis (NTA)

Isolated EV pellets were re-suspended in PBS which had been pre-filtered through a 0.2 μm membrane. A Malvern NanoSight NS300 was used to determine particle count and mean/mode particle sizes. Samples were diluted until within the range of 30–100 particles per frame. Each sample was run in triplicate and the average was taken. Matching samples (i.e., pre/post-fasting from the same subject) were extracted and analysed simultaneously to reduce effects of storage or variations in sample handling.

2.4 | TEM and cryoEM

Mouse EVs were visualised by a Hitachi HT7700 transmission electron microscope (TEM) at Taipei Medical University core facility, operated by a technician. Human EV samples were handled by technicians at the Academia Sinica Cryo Electron Microscope (ASCEM) core facility. Samples were vitrified using an FEI VitroBot-2 and images were acquired using an FEI Tecnai F20 system.

2.5 | Protein quantification and Western Blot

Total protein content of the serum and EV extracts were quantified by bicinchoninic acid (BCA) assay (Pierce, 23225). Western Blot was used to confirm the presence or absence of exosome markers using a commercial characterization kit (SystemBio, Exo-Ab kit 1) comprising rabbit polyclonal anti-human CD9, CD63, CD81 and HSP70 antibodies and goat anti-rabbit-HRP secondary antibodies. For Western blot 20 μg total EV protein was loaded per well into a pre-cast 10 % polyacrylamide gel (BioRad, 4568034). Images were captured using the iBright CL750 Imaging System with Bio-Rad Clarity Max substrate. Due to widely varying amounts of each protein, the exposure was independently set as appropriate to visualise each marker. For SDS-PAGE to show serum and EV protein profiles, 15 μg was loaded.

2.6 | H9C2 hypoxia reperfusion model

H9C2 rat cardiomyoblast cells were purchased from the Taiwan Bioresource Collection and Resource Centre (BCRC), product number 60096. Cells were routinely cultured in Dulbecco's Modified Eagle Medium (DMEM) with 4 mM L-glutamine, 1.5 g/L sodium bicarbonate and 4.5 g/L glucose, with 10 % (v/v) foetal bovine serum (FBS, Hyclone SH30396.03). For experiments using exogenous EVs, cells were switched to EV-depleted FBS (Thermo, A2720801) for two days prior to the experiment. Hypoxia was induced using a dual-gas incubator at 1 % O_2, 5 % CO_2 and 94 % N_2 at 37°C, with serum starvation. To induce reperfusion injury,

cells were replenished with fresh culture medium and simultaneously returned to normoxia. Timings and doses of EV treatments are described in the results section and figure legends.

2.7 | Kidney epithelial cell models

HK-2 human kidney epithelial cells were cultured in Keratinocyte Serum Free Medium (KSFM) with 6 mM L-Glutamine. For experiments, cells were maintained in DMEM F-12 with 2.5 mM L-glutamine, 1.2 g/L sodium bicarbonate and 3.2 g/L glucose, with 10 % (v/v) EV-depleted FBS. Toxic injury was induced by incubation with 30 μg/mL aristolochic acid. NRK-52E cells were routinely cultured in DMEM with 5 % (v/v) bovine calf serum.

2.8 | Cell viability testing

All cell viability was measured using a WST-based assay (CCK-8, Boster Bio AR1160). Reagent was added at 10 % (v/v) to each well using a repeating multi-well pipette and incubated for 3–6 h. Absorbance was then read at 450 nm in a multi-well reader. Blanks containing identical culture medium and CCK-8 reagent without cells were subtracted. EVs were confirmed to have no effect on CCK-8 absorbance compared to blank medium.

2.9 | Macrophage polarisation

RAW264.7 cells were purchased from BCRC, Taiwan. To induce M1 or M2-type polarisation, cells were incubated with 1 μg/mL LPS (Sigma) or 20 ng/mL IL-4 (BioLegend) for 24 h respectively. EVs from three separate human donors were added at 10 % (v/v) for 24 h. Naïve control cells were cultured in basal medium with addition of EV vehicle (10 % v/v). Macrophage polarisation was assessed by RT-qPCR using a panel of markers, show in Table S1, normalized to *Gapdh*.

2.10 | Scratch assay

Human dermal fibroblasts from a healthy female donor were purchased from BCRC, Taiwan and cultured in DMEM with 4 mM Glutamine, 1.5 g/L sodium bicarbonate and 4.5 g/L glucose. Cells were cultured in 24 well plates to approximately 90 % confluence, then treated with 10 μg/mL Mitomycin C (Sigma, M4287) for 2 h to prevent cell division. A scratch was then made using a 200 μL pipette tip and the cells were gently washed with PBS. Images were taken at 0 h, 5 h and 24 h following the scratch. The scratch area and number of cells migrating into the scratch area were calculated in ImageJ using an automated process which was applied equally to all images.

2.11 | miRNA profiling

250 μL serum from each donor was processed using ExoQuick following the manufacturer protocol. The resulting precipitate ($\sim$50 μL) was resuspended with 200 μL PBS. 700 μL QiaZol reagent (Qiagen, 79306) was added to extract RNA. A miRNA spike-in kit (Qiagen, 339390) was used as per protocol. All obtained miRNA (18 μL per sample) was transcribed to cDNA following the miRCURY LNA RT Kit (Qiagen, 339340) protocol in a single preparation for both the QC PCR and the panel PCR. For QC, 0.1 μL cDNA per well was assessed using a miRCURY LNA miRNA QC PCR Panel (Qiagen, 339331) following the protocol for serum/biofluid analysis. Quantification of all miRNAs was performed with a miRCURY LNA miRNA miRNome PCR Panel (Geneglobe ID YAHS-312YG-8), run on a Roche LightCycler 480 for 45 Cycles. For all PCR reactions, the miRCURY LNA SYBR Green PCR Kit (Qiagen, 339347) was used. Analysis was performed using the Qiagen Geneglobe website. Samples with CT values of < 36 were considered as expressed and included in the analysis. Samples were normalized to a panel of reference miRNAs (based on GeNorm), removing low-expressed miRNAs. miRNAs with a fold-change of at least two-fold in all three comparisons and adjusted *p*-value of < 0.05 (paired testing) were considered significantly different.

3 | RESULTS

3.1 | Characterising extracellular vesicles after calorie restriction in mice

After 28 days *ab libitum* feeding, the average weight of mice was 27.7 g $\pm$ 1.56 g. The average chow consumption during this 28-day period was 0.176 g per g body weight per day, which is an average calorie intake of 0.717947 kcal/g/d. To induce CR, food was provided at 70 % of the acclimatisation baseline consumption. The results (Figure 1a) show that following introduction of calorie

Calorie restriction (mouse)
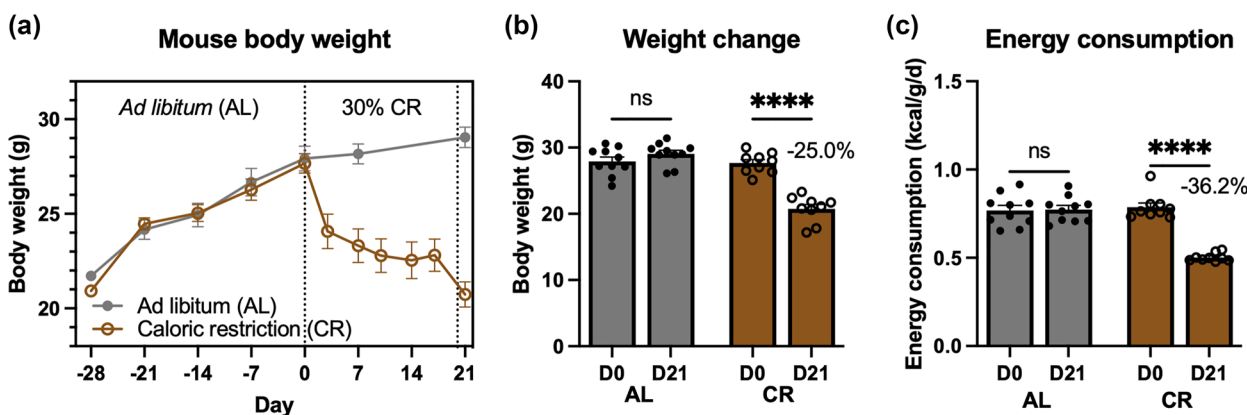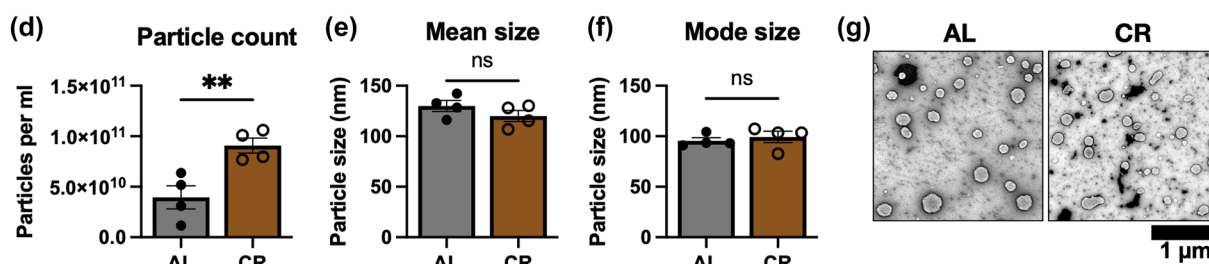

Extracellular vesicles (mouse)

FIGURE 1 (a) Timeline of mouse body weight changes during *ad libitum* (AL) feeding and after 21 days of 30% calorie restriction (CR). The dotted line at D0 shows initiation of the CR protocol. The dotted line at D20 shows the overnight water-only calorie restriction. (b) Comparison of D0 and D21 body weight for AL ($n = 10$) and CR ($n = 9$) mice. Samples were compared by one-way ANOVA, D0 versus D21. (c) Average energy consumption, determined by overall food weight changes, at D0 to D21 for AL and CR mice. (d) Mean particle count by nanoparticle tracking analysis (NTA) showing extracts from $n = 4$ mice per group. Compared by unpaired *t*-test. (e) Mean particle size determined by NTA. (f) Mode particle size determined by NTA. (g) Representative transmission electron microscopy (TEM) images of EVs from AL and CR mice. Scale bar 1 μm. ns, not significant; **$p \leq 0.01$, ****$p \leq 0.0001$.

restriction (CR), the CR group lost weight within the first 4 days, which continued at a slower rate until the end of the experiment. Statistical comparison of body weight (Figure 1b) at D0 (immediately prior to CR induction) and D21 (day of sacrifice) shows that CR mice lost, on average, 25.0 % of their body weight. Daily energy intake (Figure 1c), determined by measuring the weight of food consumed, was reduced by 36.2 % in the CR group. The *ad libitum* group did not change significantly.

Circulating extracellular vesicles (EVs) were isolated and samples from four mice per group were analysed by nanoparticle tracking analysis (NTA). As shown in Figure 1d, the total mean particle count was significantly higher in the CR group. The mean particle size (Figure 1e) and mode particle size (Figure 1f) were unchanged. Conventional TEM (Figure 1g) revealed spherical, membrane-bound particles of approximately 100 nm, with morphology typical of exosomes isolated by ExoPure preparation (Brennan et al., 2020). Unfortunately, we lacked enough sample quantity to carry out Western Blotting for mouse EV samples. However, the commercial EV isolation reagents we used are well-validated by other labs and confirmed to successfully isolate circulating EVs (Helwa et al., 2017; Huang et al., 2013).

3.2 | Examining hypoxia protective properties of murine extracellular vesicles

As described earlier, previous animal studies have shown beneficial effects of CR prior to ischaemia. Therefore, to detect any potential changes in function of the isolated EVs, a H9C2 rat cardiomyoblast hypoxia/reperfusion (H/R) injury model was used. A schematic of the experimental design is shown in Figure 2a. After 48 h of hypoxia, cell viability was significantly reduced (60.56 %) compared to the normoxia group, as shown in Figure 2b. Cells were then returned to normoxia to induce H/R injury, resulting in oxidative stress and further reduction in cell viability. Upon reoxygenation, cells were incubated with 10 % FBS (Pos) or serum-free media (Neg) as positive and negative controls respectively. FBS was able to buffer against reperfusion injury and cell metabolic activity fell to 39.9 % compared to 6.3 % for cells without serum. Cells incubated with a 10 % (v/v) suspension of *ad libitum*-derived EVs had higher viability (14.8 %) than the negative control. However, cells incubated with CR-derived EVs had 37.1 % viability, which was significantly higher than the AL EV group. Inspection of cell morphology (Figure 2c) showed that
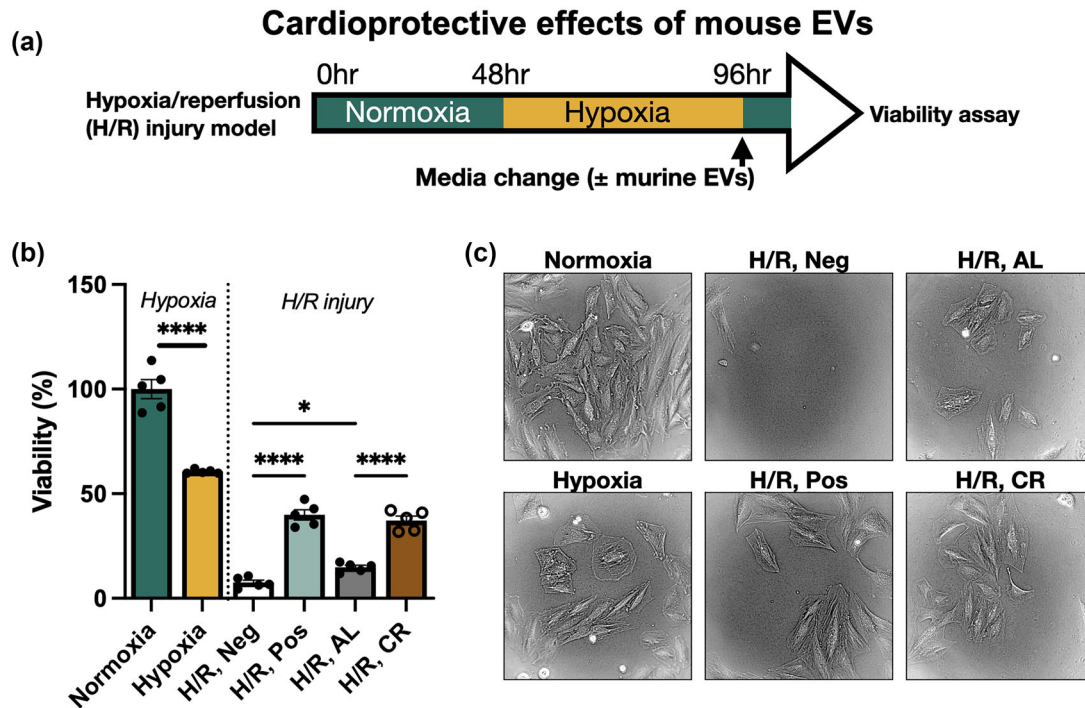
FIGURE 2 (a) Schematic diagram of *in vitro* H9C2 hypoxia/reperfusion (H/R) injury experiment. (b) Viability of H9C2 rat cardiomyoblasts after 48 h hypoxia, and H/R with 0 % FBS (Neg), 10 % FBS (Pos), 10 % *ad libitum*-derived EVs (AL) or 10% calorie restriction-derived EVs (CR). Samples were compared by ANOVA with Tukey's post-test. (c) Representative images of H9C2 cells are shown for each condition. $*p < 0.05$, $****p \leq 0.0001$.

TABLE 1 Donor characteristics prior to water-only fasting

Donor	Age (years)	Sex	Height (cm)	Weight (kg)	BMI (kg/m^2)	Duration (h)
1	34	F	160	56.0	21.8	108
2	35	M	171	78.9	26.9	84
3	46	M	183	87.1	26.0	84
4	27	M	170	65.0	22.4	84
5	28	F	157	62.1	25.1	84
6	23	M	176	86.6	28.0	84
7	31	M	175	65.6	21.4	84
8	32	F	169	71.0	24.9	84

H9C2 cells in the injury groups displayed swollen morphologies and a lower cell number than the normoxic control. The H/R CR EV group showed a greater cell number than the AL EV group, and cell morphology was more similar to the Pos group. Taken together, these results indicate that circulating EVs from calorie restricted mice appeared to have greater protective properties than those from *ad libitum*-fed mice.

3.3 | Characterising extracellular vesicles after water-only fasting in human donors

Since the mouse experimental results showed proof-of-principle that EVs derived after CR would have hypoxia-protective properties, we sought to carry out a similar experiment in humans. A prolonged 30 % calorie restriction in humans would require resources beyond the capability of our lab. However, studies have shown that short periods of low calorie intake have long-lasting metabolic benefits in healthy weight individuals (Wei et al., 2017). Circulating IGF-1 and inflammatory markers were also reduced, demonstrating that even a short period of fasting can alter systemic circulating factors. Therefore, we recruited human donors and obtained blood samples before and after a period of water-only fasting, as shown in Figure 3a. **Table 1** shows the donor characteristics.

Water-only fasting (human)

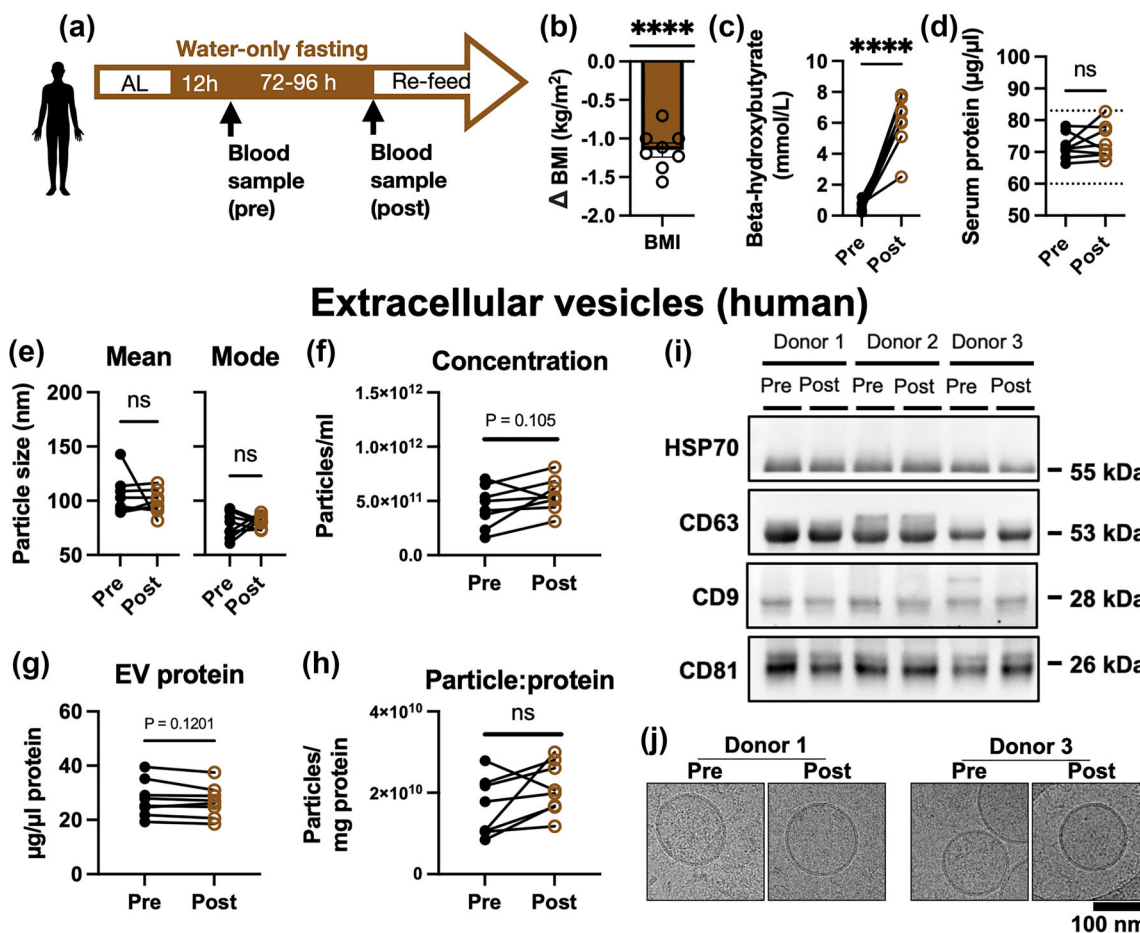## Extracellular vesicles (human)

FIGURE 3 (a) Schematic of human fasting experimental design. (b) Mean change in body mass index (BMI) from pre- to post- fasting samples. $N = 8$ donors. Compared by one-way t-test versus a mean change of 0. (c) Serum beta hydroxybutyrate (BHB, ketone) levels. (d) Serum total protein concentration. The Y axis dotted lines show the standard reference range. Compared by paired t-test. (e) Mean and mode EV size determined by nanoparticle tracking analysis (NTA). (f) Particle concentration of EV extracts determined by NTA. (g) EV protein concentration determined by BCA assay. (h) Serum EV particle to protein ratio. Samples from the same subject pre- to post-fasting are joined by a line and were compared by paired t-test. Pre- versus post-fasting samples were compared by paired t-test. (i) Western blot of exosome markers HSP70, CD63, CD9 and CD81 for three separate donors. Exposure length was adjusted to enable visualisation, depending on the strength of each marker. (j) cryoEM of EVs derived from pre- and post-fasting samples of two human donors. ****$p \leq 0.0001$, ns, not significant.

Figure 3b shows the change in BMI for each subject. All subjects lost ≥ 3.0 kg total body weight, with an average reduction in BMI of -1.14 kg/m² which was highly significant (one sample t-test, $p \leq 0.0001$). Subject samples were tested for beta hydroxybutyrate (BHB) levels pre-/post-fasting (Figure 3c). Serum BHB increased from an average of 0.51 ± 0.13 mmol/L pre-fasting to 6.08 ± 0.60 mmol/L post-fasting ($N = 8$, $p \leq 0.0001$ by paired t-test), demonstrating that the subjects were in a robust state of ketogenesis (Newman & Verdin, 2014). This supports good overall compliance with the fasting protocol. Total serum protein was also measured for all samples (Figure 3d), and showed no significant difference after fasting ($p = 0.41$, $N = 8$, paired t-test). All samples were within the normal reference range for healthy humans. Serum EVs were isolated and characterised by NTA. There was no significant difference between the mean or mode particle size of the pre/post-fasting samples, as shown in Figure 3e. Average particle concentration after fasting (Figure 3f) was not significantly different, nor was protein EV content (Figure 3g). Calculating the ratio of particle number to protein concentration (Figure 3h) showed no significant difference between groups, indicating that the purity of each isolation was similar, and not contaminated by excess non-EV particles, or excess free proteins. Total protein extracts from three donors were analysed by SDS-PAGE (Figure S1, S2). The results showed no noticeable changes in the overall protein profile of serum or EV isolated between pre- and post-fasting samples. Western Blot (Figure 3i) was used to determine whether the isolated particles expressed markers HSP70, CD63, CD9 and CD81. Samples from three donors, both before and after fasting, were positive for all markers. Lastly, cryoEM (Figure 3j) was used to observe the structure of the isolated particles. In pre- and post-fasting samples from two donors, spherical, ~100 nm vesicles with lipid bilayers were detected. Taken
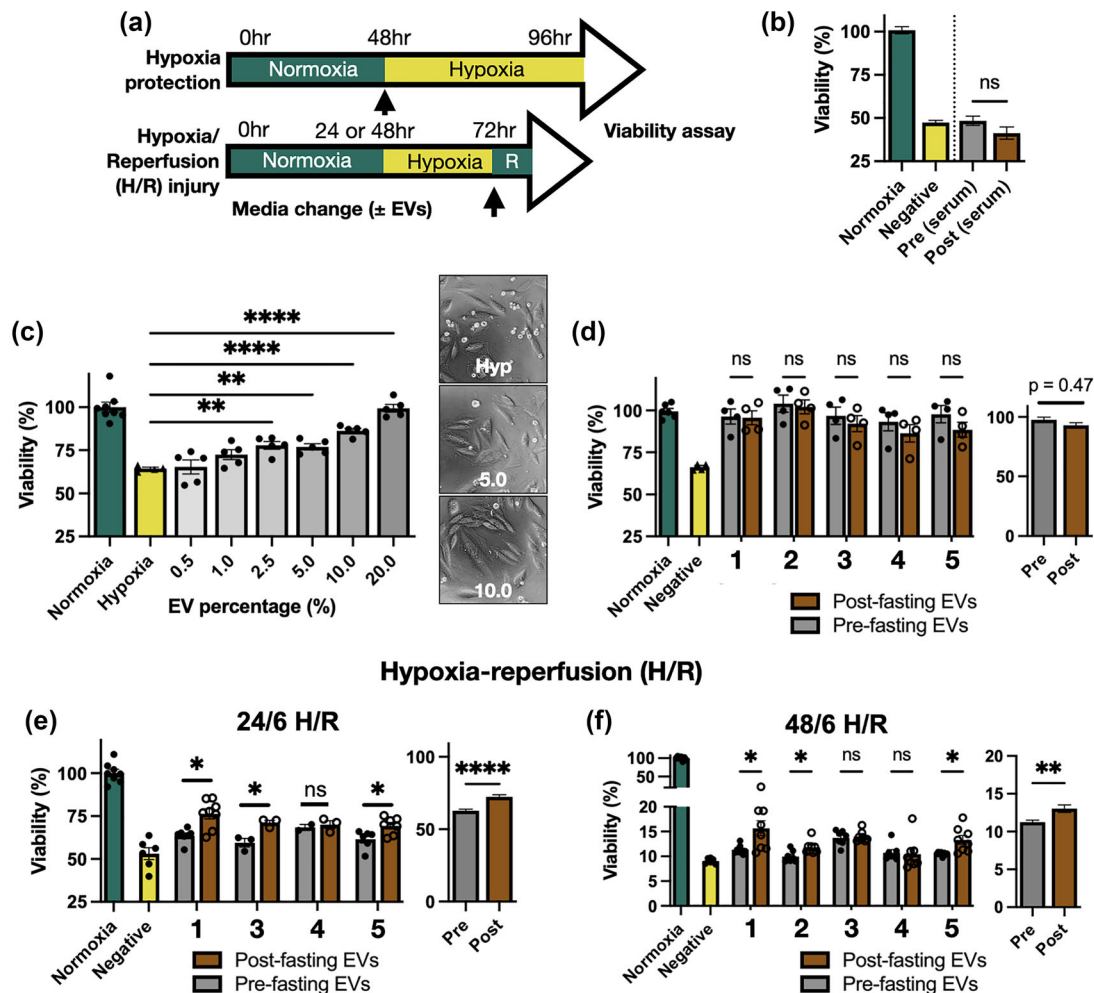

FIGURE 4 (a) Schematic of H9C2 hypoxia protection and hypoxia/reperfusion (H/R) assays. $R = 6$ h reperfusion. (b) Effect of 0 % FBS (Negative), or 10 % pre- or post-fasting human serum on H9C2 viability during hypoxia. $N = 2$ donors, 3 replicates per sample. (c) Dose-response of EVs by % volume. EVs were from one donor (Subject 1, pre-fasting) and each dot shows one replicate. Samples were compared to negative control by one-way ANOVA. (d) Effect of 10% (v/v) EV concentration on H9C2 hypoxia protection, from five donors. Pre- and post-fasting samples were compared by two-way ANOVA for each donor, and the overall effect was calculated by nested t-test. (e) H9C2 viability after 24/6 h H/R injury with EVs from four donors. (f) H9C2 viability after 48/6 h H/R injury with EVs from five donors. ns, not significant, $^*p < 0.05$, $^{**}p \leq 0.01$, $^{***}p \leq 0.001$, $^{****}p \leq 0.0001$.

together, these data confirm that serum EVs were successfully purified. Since the biogenesis of the vesicles cannot be known, we will continue to refer to them as EVs rather than "exosomes."

3.4 | Examining hypoxia protective properties of human extracellular vesicles

Human blood-derived EVs are known to be cardioprotective in *in vitro* cultured rat cardiomyocytes and rat MI models (Vicencio et al., 2015). Therefore, we used two H9C2 cell hypoxia protocols to mimic myocardial infarction injury, as shown in Figure 4a. First, we used a simple hypoxia protection model where cells were subjected to 48 h hypoxia in the presence of each treatment condition. As an initial test, cells were cultured in media supplemented with 10 % (v/v) of the whole human serum from pre- and post- fasting samples. These were compared to serum-free conditions (Negative). Viability testing (Figure 4b) found that whole human serum from two donors, (subject 1 and subject 3, provided at 10 % v/v) had no significant beneficial effect on the cells; nor was there any difference between pre- and post-fasting serum.

Next, we tested the purified EVs. To establish a working dose range for future experiments we supplemented hypoxic H9C2 cells with purified EVs (from subject 1, using pre-fasting samples) at concentrations ranging from 0.5 to 20 % (v/v). EV-supplemented cells under hypoxia were compared to cells cultured under normoxia. The results (Figure 4c) showed that concentrations above
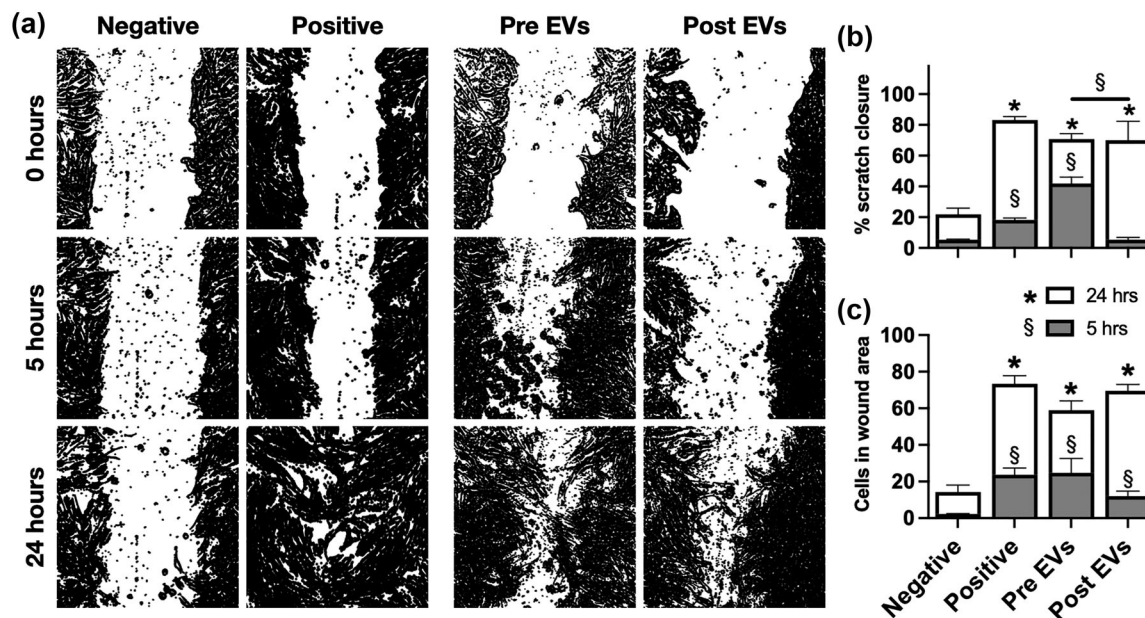
Scratch cell migration assay

FIGURE 5 (a) Visualisation of scratch assay closure at 0, 5 and 24 h. The images were generated by an automated procedure in ImageJ. The white area signifies the scratch. (b) Scratch wound area percentage remaining after 5 and 24 h. (c) Number of cells inside the wound area after 5 and 24 h. Groups were compared by two-way ANOVA. § shows comparisons at 5 h (grey bars) and * shows comparisons at 24 h (white bars). Error bars show standard error of the mean from $N = 3$ separate EV donors.

2.5 % (v/v) EVs had a significant protective effects on the H9C2 cells. The example images show that EV-supplemented cells had improved morphology and a greater cell number. To balance effectiveness with conservation of our limited sample volumes, we opted to use 10 % (v/v) for our further experiments. This is equal to a final concentration of approximately 2.7 μg/μL of EV protein, or 5×10^7 particles/μL.

We then tested hypoxia protection using five separate donor EV samples at 10 % (v/v). The results (Figure 4d) showed that all groups containing EVs showed higher cell viability than the negative control, demonstrating that all of the human EV samples had hypoxia-protective effects. It is interesting to note that the isolated EVs were beneficial but the whole serum (Figure 4b) was not, despite the whole serum having a much higher total protein content. Assessing all samples together by nested t-test produced a p-value of 0.466, summarised in the adjacent graph. Thus, we conclude that there was no significant difference between pre- and post-fasting EVs in this hypoxia protection assay.

Next, we used the H/R model where all cells were subjected to 24 h hypoxia and serum deprivation, then restored to normoxia with simultaneous addition of 10 % (v/v) EVs. Viability was measured at 6 h following restoration of normoxia. The results from four separate donors (Figure 4e) show that H/R reduced cell viability (53.1%), as expected, and addition of human EVs significantly preserved cell viability compared to the negative control. In this assay, EVs derived from donors post-fasting preserved significantly higher cell viability than pre-fasting EVs in three out of the four donors tested. The overall average viability of cells treated with pre-fasting EVs was 62.0 %, which increased to 72.4 % with post-fasting EVs. Comparison by nested t-test showed that this was highly significant, with a p-value of 0.006. A more severe injury model using 48 h hypoxia and 6 h normoxia (Figure 4f) reduced cell viability of the vehicle control (negative) group to only 9.6%. Addition of EVs at the time of reperfusion produced slightly increased viability, with post-fasting EVs producing a slightly higher average (13.0 %) than pre-fasting EVs (11.1 %). This was statistically significant for three of five donors, and nested t-test of all pre- versus post-fasting EVs gave a p-value of 0.003. Overall, these findings show that human circulating EVs may have improved cardioprotective potential following fasting. However, the difference was moderate and not consistent between all donors.

To avoid drawing conclusions from a single cell line, we utilised a human kidney proximal tubule epithelial cell line, HK-2. Kidney ischaemia causes apoptosis or necrosis of renal epithelial and endothelial cells, resulting in chronic kidney disease (CKD) or acute kidney failure (Sharfuddin & Molitoris, 2011). HK-2 cells are a well-known model for kidney hypoxia (Andrade-Oliveira et al., 2015). Using a 48/6 H/R protocol (Figure S3a), EVs from both pre- and post-fasting samples were provided at doses from 0.1 to 20.0 % (v/v). The viability results (Figure S3b,c) showed that the H/R protocol reduced HK-2 viability to an average of 57.49 % compared to normoxia. However, there was no significant protective effect of human serum-derived EVs, even at 20 % (v/v) concentrations. Furthermore, there was no difference between pre- and post-fasting EVs. We were surprised by this

negative result and wondered whether this was specific to the H/R injury model, or if the kidney epithelial cells themselves were unresponsive to the EVs. CR (40 %) has been demonstrated to protect the rat kidney from drug-induced injury nephrotoxicity (Ning et al., 2014). Therefore, we utilised aristolochic acid (AA), which is a potent nephrotoxic agent, to induce HK-2 injury (Lu et al., 2021). Addition of 30 μg/mL AA for 24 h reduced HK-2 viability to approximately 40 %. AA was then removed and EVs from five donors were added at 10 % (v/v). Again, this showed no significant effect on enhancing cell viability (Figure S3d). We additionally tested another kidney epithelial cell line, NRK-52E, which also showed no response to supplemental EVs following H/R injury (Figure S3e). Overall, the supplemental EVs had no effect on kidney epithelial cell viability in hypoxic or toxic injury models.

3.5 | Examining stimulation of cell migration by extracellular vesicles from fasted humans

Following myocardial infarction or kidney injury, resident fibroblasts migrate to the injured site (Shi et al., 2017). Previous studies have shown that stem cell-derived EVs can influence cell motility in ischaemic injury (Gangadaran et al., 2017). Therefore, we used a dermal fibroblast wound-healing assay to measure any potential differences in the ability of pre- and post-fasting EVs to stimulate cell migration. Primary human dermal fibroblasts were grown to confluence and the cell cycle was arrested by Mitomycin treatment. After the scratch was created, cells were incubated with serum-free culture medium containing EVs from donors three, four or five (10 % v/v), or EV vehicle (negative control) for 24 h. Medium containing FBS was included as a positive control. Representative images, processed by ImageJ, are shown in Figure 5a. Both pre- and post-fasting EVs stimulated cell migration compared to the negative control, at 5 and 24 h. However, the results showed that, on average, post-fasting EVs had slower scratch closure and less cells migrating into the wound area than those treated with pre-fasting EVs (Figure 5b,c). After 24 h, the overall results from both EV groups were similar.

3.6 | Examining macrophage polarisation by extracellular vesicles from fasted humans

Previous studies have shown that CR or fasting may induce immunomodulation—particularly the suppression of inflammation (Harvey et al., 2014). This, in turn, may reduce tissue injury following ischaemia. Ketones, increased following CR, have been shown in isolation to reduce NLRP3 inflammasome signalling in macrophages (Youm et al., 2015). Therefore, we hypothesised that fasting-derived EVs may differentially affect macrophage polarisation. To test this, we used the RAW246.7 macrophage cell line. As controls, lipopolysaccharide (LPS) was used to induce an "M1-like" phenotype and interleukin-4 (IL-4) was used to induce an "M2-like" phenotype. A panel of primers (Table S1) was then used to then assess polarisation-related gene expression after 24 h (Figure 6a). The results, (Figure 6b) show the log2 fold change for each condition compared to the relevant control condition. LPS (red bars) and IL4 (yellow bars) were compared to macrophages incubated with the EV vehicle. Post-fasting EVs were compared to pre-fasting EVs alone (brown bar). Lastly, we tested pre- and post-fasting EVs in the presence of LPS (grey bars). The results showed that LPS induced M1 markers, particularly *Il1b*, *Nos2* and *Il6*. *Arg1*, *Tnfa* and *Il10* were also increased. IL4 increased M2 markers including *Arg1 and Irf4*, and suppressed *Il6*. The RAW246.7 cells did not show changes in *Nlrp3* gene expression following any treatment. The effects of pre- versus post-fasting EVs from three separate donors (donors one, three and four) on otherwise non-stimulated RAW246.7 cells, are shown by the brown bars. The results show that post-fasting EVs induced less *Il10*, *Il6* and *Il1b* than pre-fasting EVs, and induced more *Retnla* expression. There were no differences in the effect of pre/post-fasting EVs on *Nos2*, *Arg1* or *Irf4* expression. This indicates a trend towards a reduced inflammatory phenotype, but the EVs did not induce a distinct "M1" or "M2" signature and overall changes in gene expression were mild.

We then tested whether EVs may affect inflammatory markers in the presence of pro-inflammatory signalling. RAW246.7 cells were treated with low dose LPS alongside 10 % (v/v) pre or post-fasting EVs, shown by the grey bars. Interestingly, the results showed that cells incubated with post-fasting EVs showed significantly lower expression of *Il6, Tnfa* and *Nos2* compared to pre-fasting EVs. There was also a trend towards reduced *Il1b* but one donor produced particularly large reductions in expression which increased the intra-sample variability. Therefore, the results of this experiment indicate that post-fasting EVs may have anti-inflammatory properties, although they did not produce a clear-cut "M2" phenotype or suppress all inflammatory markers.

3.7 | Examining miRNA cargo of extracellular vesicles from fasted humans

Lastly, we sought to examine whether the EV miRNA cargo differed between pre- and post-fasting samples. We utilised a PCR-based array to specifically detect 752 known miRNAs from EVs obtained from three subjects (donors six, seven and eight) before and after 72 h fasting. As shown in Figure 7a, 55 % to 61 % of surveyed miRNAs were detected in all samples with CT values of less

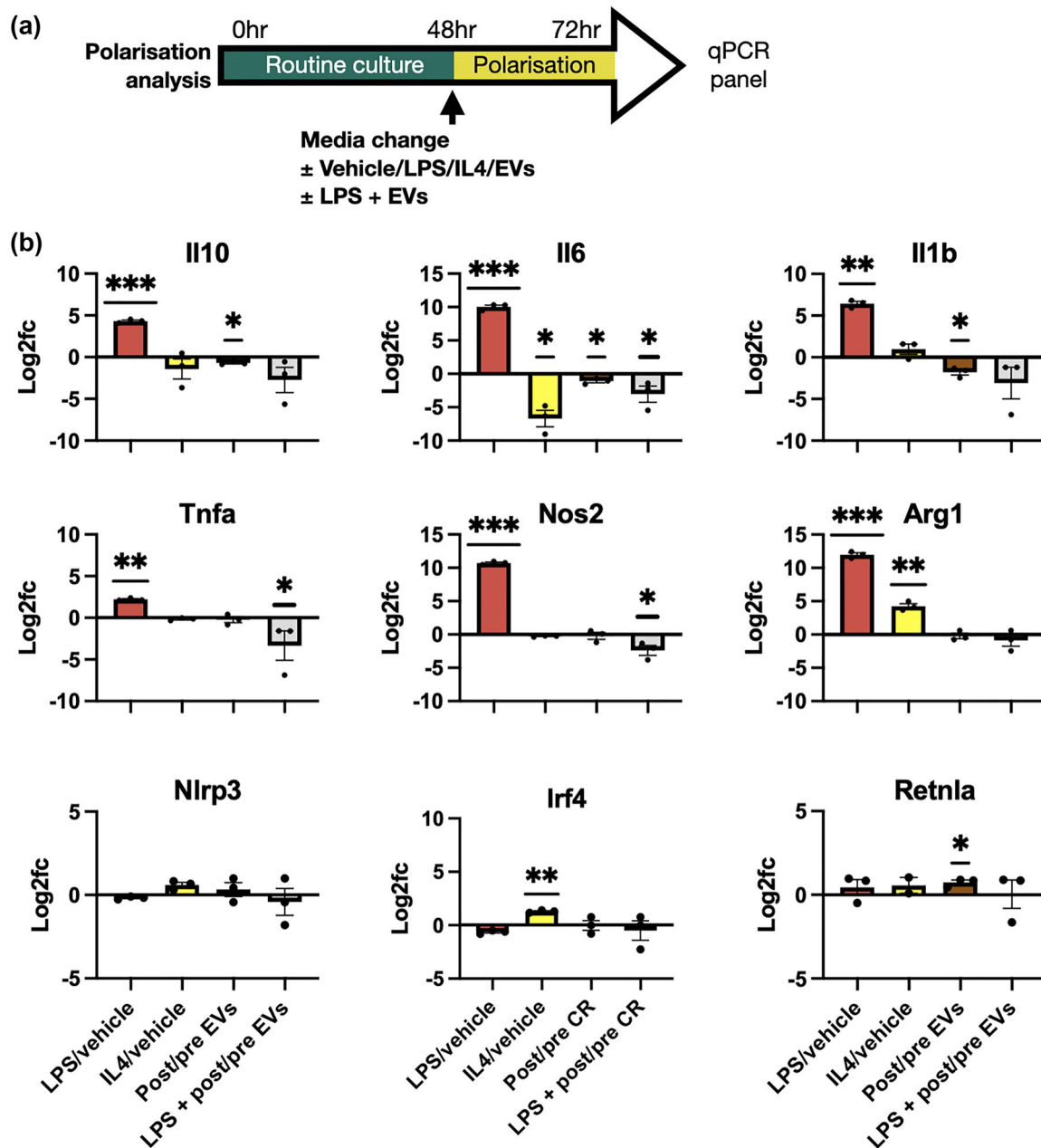# Macrophage polarisation assay

FIGURE 6 (a) Schematic diagram showing experimental timelines. (b) Assessment of macrophage polarisation markers after 24 h incubation with lipopolysaccharide (LPS), Interleukin 4 (IL4), or EVs from pre- or post-fasting donor samples. Each graph shows log2 fold change versus the relevant control. For LPS (red) and IL4 (yellow), the fold change compared to non-stimulated macrophages is shown. The brown bars show differential effects of pre- and post-fasting EVs on naive macrophages. The grey bar shows pre- and post-fasting EVs on LPS-stimulated macrophages. Three individual donor EVs samples are shown by dots, and each donor had three replicates. To determine statistical significance samples were compared by one-way t-test against a hypothesised fold change of zero. $*p \leq 0.05$, $**p \leq 0.01$, $***p \leq 0.001$.

than 36.0. Quality control data (Figure S4) shows successful amplification of spiked-in UniSP2, 4 and 5, detected at CT values of 21.1, 28.9 and 33.8, representing high, medium and low expression respectively. There was also excellent cross-sample consistency (CT = 19.74 ± 0.08) based on inter-plate calibration wells (UniSP3). Together, these results show that miRNA extraction, reverse transcription and amplification was successful.

Principal component analysis (PCA) showed that pre-fasting and post-fasting miRNA expression profiles had relatively distinct groupings (Figure 7b). A scatter graph (Figure 7c) shows pre- (Y axis) versus post-fasting (X axis) EV miRNA expression levels normalised to geNorm reference miRNAs. The most abundant miRNAs detected were miR-451a, miR-223-3p and
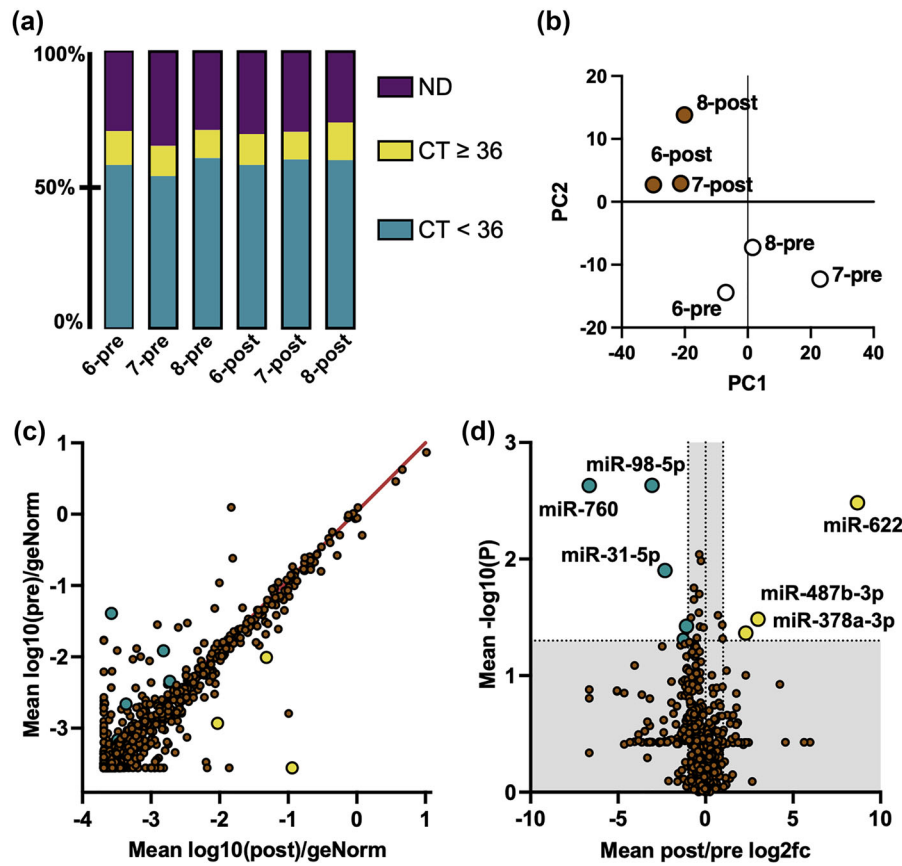
EV miRNA analysis

FIGURE 7 Comparison of miRNA cargo extracted from pre- and post-fasting EVs. (a) Percentage of 752 total miRNAs detected with cycle threshold (CT) values of <36, ≥36, or not detected (ND) for each sample. Samples with CT ≤ 36 in all six samples were included in the following analyses. (b) Principal component analysis (PCA) of all samples. Pre-fasting EV samples are shown in white, and post-fasting EV samples are shown in brown. (c) Scatter plot showing mean expression level, normalised to reference miRNAs, for pre-fasting (Y axis) and post-fasting (X axis) miRNAs. The red line shows a reference gradient of 1. Statistically significant results are highlighted green (reduced in post-fasting) and yellow (increased in post-fasting). (d) Volcano plot showing fold change (X axis) and statistical significance (Y axis). The Y axis grey area shows $p > 0.05$ and X axis grey area shows fold-change <2.0. Statistically significant results are annotated.

miR-16-5p, which are all well-known serum EV cargo (Helwa et al., 2017). A list of the 25 most abundant miRNAs is shown in Table S2. A volcano plot (Figure 7d) showing fold change (X axis) and p-values (Y axis) revealed a small number of statistically significant changes between pre- and post-fasting miRNAs. The significantly upregulated miRNAs were miR-622, miR-487b-3p and miR-378a-3p and the downregulated miRNAs were miR-760, miR-98-5p and miR-31-5p. Exact fold changes and p-values are shown in Table S3. Target prediction using DAVID did not show any common biological pathway for the three upregulated miRNAs, however, the Geneglobe prediction service highlighted several potential gene interactions, shown in Table S4.

Surveying the literature surrounding these miRNAs revealed several interesting findings. miR-622 has been directly shown to reduce expression of the enzyme RNF8 and increased miR-622 increased the rate of cellular DNA damage repair and slowed cell migration (Liu et al., 2019). The second upregulated miRNA, miR-487b-3p, has been previously shown, in rats, to be linked to ageing (Lee et al., 2018). In terms of function, miR-487b-3p has been shown to act on the IGF-1 signalling pathway in muscle tissues (Wang et al., 2018). It has also been shown to regulate macrophage IL-33 expression, whereupon increased miR-487b-3p lowered the macrophage pro-inflammatory response to LPS stimulation (Xiang et al., 2016). These findings support our findings that post-fasting EVs appeared to reduce macrophage pro-inflammatory response and reduced cell migration. Interestingly, the third upregulated miRNA we detected, miR-378, has been shown to play roles in energy homeostasis, mitochondrial function, oxidative capacity and the response to metabolic stress (Carrer et al., 2012).

Taken together, the results of our study show that CR and fasting appear to induce changes in the properties of circulating EVs in both mice and humans. The isolated EVs showed moderate, though sometimes inconsistent, differences in their effects when tested in *in vitro* assays. In particular, post-fasting EVs were superior to pre-fasting EVs at protecting cardiac cells from

hypoxia/reperfusion injury. In terms of wound healing, post-fasting EVs stimulated less fibroblast migration than pre-fasting EVs, in our assays. Lastly, we found that post-fasting EVs tended towards reducing pro-inflammatory signalling in macrophages.

4 | DISCUSSION

Fasting has been shown to confer many measurable health benefits, including protection from hypoxic injury, in multiple animal models. Since EVs vary by donor properties, including health/disease status, we hypothesised that EVs isolated from fasted subjects may also confer those benefits. Previous studies have shown alterations in serum EVs miRNAs due to CR in animals, though these studies did not look at efficacy/function of the EVs (Lee et al., 2018; Liu et al., 2020). These rodent studies rely on longer periods of CR; typically 30 % to 40 % restriction, maintained for at least several weeks. Our animal study was designed in the same manner, subjecting mice to 21 days of a 30 % calorie deficit. Our mouse study results (Figures 1 and 2) found that circulating EVs from calorie-restricted C57BL/6 mice did appear to have improved cardioprotective properties in an *in vitro* model of hypoxia.

However, there are many differences between the rodent and human responses to CR/fasting, which limit the comparisons that can be made between the two species. For example, the progression of weight loss in rodents and humans differs significantly. Standard laboratory mice are typically much leaner than average humans, enter ketosis and gluconeogenesis faster than humans, and experience more rapid weight loss than humans (up to 20 % of their body weight after 24 h of water-only fasting) (Boldrin et al., 2017). Therefore, results from rodent CR protocols do not necessarily translate to results in humans (Ingram and de Cabo, 2017). For example, one human clinical trial investigated whether seven days of 40 % CR would provide renal protection following scheduled cardiac surgery, but did not find any measurable benefit (Grundmann et al., 2018).

In our study we sought to focus primarily on samples derived from humans. This necessitated changing the dietary protocol, since recruiting subjects to a long-term diet program and ensuring their compliance and safety is beyond the capability of our research group. A short (3–5 day) period of water-only fasting was a feasible strategy to accomplish this since previous human studies have shown long-lasting metabolic changes can be induced from 72 h of low calorie diet (Cheng et al., 2014; Wei et al., 2017).

However, this short duration is a limitation of our study. Changes in EV properties can be initiated quickly, such as after acute injury or with one night of sleep deprivation (Luo et al., 2023; Wang et al., 2022). However, we speculate that a longer fasting period (under appropriate clinical supervision) would allow more time for the circulating EV pool to be turned over. Another caveat is that, by necessity of IRB approval for our study design, we recruited normal weight, young adults who were metabolically healthy and absent of chronic diseases. It is plausible that metabolically dysfunctional individuals would show greater changes in circulating EVs following fasting. However, such subjects would require closer clinical supervision or in-patient monitoring which our lab is unable to provide.

Our results from the RAW246.7 cell line support previous studies of CR, aging and macrophage function. For example, macrophages derived from aged, calorie-restricted mice showed reduced *Il6*, *Il10 Tnfa* and *Il1b* expression following LPS stimulation (Vega et al., 2004). Our study showed that EVs derived from post-fasting human donors attenuated macrophage expression of these markers when stimulated by LPS. This implies that some degree of the immunomodulatory effects of CR/fasting may be derived by circulating EVs acting on immune cells. Our EV cargo miRNA analysis also detected increased concentrations of miRNAs with anti-inflammatory activities. In the future, we hope to use *in vivo* models to assess whether post-fasting EVs could affect macrophage polarisation in injured tissues, and whether this has subsequent effects on parenchymal cells.

There are some methodological factors and limitations to consider when interpreting our results. Extracellular particles (EPs) are complex biological products and there is no single preferred method for their purification or characterisation. Phospholipid bilayer membrane-bound EVs are one population of EP, which includes microvesicles, exosomes and apoptotic bodies. Exosomes are a specific subset of EVs, defined by their mechanism of biogenesis and secretion, as well as surface markers. Isolation of EVs from blood plasma, blood serum, urine, CSF or other fluids each have different best practices for their handling and preparation (Lai et al., 2022; Théry et al., 2018). For example, serum contains an additional portion of EVs derived from platelet activation during blood coagulation, which may be desired or undesired, depending on the application. Platelet-derived EVs themselves have been shown to contain pro-regenerative cargos and have protective properties (Widyaningrum et al., 2021). Since we could only obtain limited sample volumes, we opted to trade higher purity in favour of greater yield, which would thus allow us to carry out more experiments. To do this, we used commercial exosome isolation kits which are well-validated by a large body of prior literature (Helwa et al., 2017; Lai et al., 2022; Théry et al., 2018). Following EV isolation, NTA showed a single peak with a mean diameter < 150 nm, western blot confirmed several common exosome markers, and cryoEM showed vesicles formed from lipid bilayer membranes. Together, this provides strong evidence that we successfully isolated circulating EVs. However, these blood-derived samples likely also include other nanoscale particles such as chylomicrons, lipoproteins (LDL, HDL, VLDL etc.), protein aggregates or cell fragments, as well as free proteins (Brennan et al., 2020). Knowing this would be the case, we ensured that the pre-fasting samples were still taken after an overnight fast to reduce excessive contamination of chylomicrons or products of digestion. Baseline BHB levels of 0.51 mmol/L indicate good compliance with the overnight fasting. In addition,

SDS-PAGE analysis showed no missing or additional protein bands in the post-fasting serum or EV samples, and the particle:protein ratio was consistent between samples. Nevertheless, it is possible that alternative exosome isolation methods could produce different results due to selection of alternative EV subpopulations. For example, size exclusion chromatography can collect specific fractions of EVs and free proteins which can be separately examined (Lai et al., 2022) We elected not to carry out further purification or fractionation because we aimed to assess the "whole picture" of the effects of calorie restriction, and we could only acquire limited sample volumes. In the future we hope to recruit more human subjects and to carry out more detailed analyses.

Lastly, our study focused mainly on ischaemic disease models, but EVs, and CR/fasting as treatment modalities, have been explored for many other purposes including protection from toxins, prevention of neurodegeneration, or as drug delivery vehicles (Agrahari et al., 2019; Osorio-Querejeta et al., 2020; Soler-Botija et al., 2022). Thus, is possible that fasting-derived EVs may have differential effects in other models. It is also likely that some functional differences may not manifest in *in vitro* models. In the future we hope to carry out *in vivo* studies to address these questions and to investigate the downstream mechanisms of action.

AUTHOR CONTRIBUTIONS

Manuel S.V. Jaimes: Investigation (Figures 3–7), validation, visualisation, writing—original draft. **Chia-Te Liao**: Resources, recruited subjects, supervision, conceptualisation, administration, writing—review and editing. **Max M. Chen**: Investigation (Figures 1–2), validation. **Andreas Czosseck**: Investigation (Figure 7), writing—original draft. **Tsung-Lin Lee**: Investigation (kidney epithelial cell AA model). **Yu-Hsiang Chou**, **Yung-Ming Chen** and **Shuei-Liong Lin**: Resources, Methodology. **James J. Lai**: Conceptualisation, supervision. **David J. Lundy**: Funding, conceptualisation, project administration, supervision, writing—review and editing, recruited subjects.

ACKNOWLEDGEMENTS

CONFLICT OF INTEREST STATEMENT

There are no conflicts of interest to declare.

ORCID

David J. Lundy https://orcid.org/0000-0003-0848-3206

REFERENCES

Agrahari, V., Agrahari, V., Burnouf, P. A., Chew, C. H., & Burnouf, T. (2019). Extracellular microvesicles as new industrial therapeutic frontiers. *Trends Biotechnol*, *37*, 707.

Andrade-Oliveira, V., Amano, M. T., Correa-Costa, M., Castoldi, A., Felizardo, R. J. F., de Almeida, D. C., Bassi, E. J., Moraes-Vieira, P. M., Hiyane, M. I., Rodas, A. C. D., Peron, J. P. S., Aguiar, C. F., Reis, M. A., Ribeiro, W. R., Valduga, C. J., Curi, R., Vinolo, M. A. R., Ferreira, C. M., & Câmara, N. O. S. (2015). Gut bacteria products prevent AKI induced by ischemia-reperfusion. *Journal of the American Society of Nephrology*, *26*, 1877.

Barile, L., Lionetti, V., Cervio, E., Matteucci, M., Gherghiceanu, M., Popescu, L. M., Torre, T., Siclari, F., Moccetti, T., & Vassalli, G. (2014). Extracellular vesicles fromhuman cardiac progenitor cells inhibit cardiomyocyte apoptosis and improve cardiac function aftermyocardial infarction. *Cardiovascular Research*, *103*, 530.

Barile, L., Moccetti, T., Marbán, E., & Vassalli, G. (2017). Roles of exosomes in cardioprotection. *European Heart Journal*, *38*, 1372.

Boldrin, L., Ross, J. A., Whitmore, C., Doreste, B., Beaver, C., Eddaoudi, A., Pearce, D. J., & Morgan, J. E. (2017). The effect of calorie restriction on mouse skeletal muscle is sex, strain and time-dependent. *Scientific Reports*, *7*, 5160.

Brennan, K., Martin, K., FitzGerald, S. P., O'Sullivan, J., Wu, Y., Blanco, A., Richardson, C., & Mc Gee, M. M. (2020). A comparison of methods for the isolation and separation of extracellular vesicles from protein and lipid particles in human serum. *Scientific Reports*, *10*, 1.

Carrer, M., Liu, N., Grueter, C. E., Williams, A. H., Frisard, M. I., Hulver, M. W., Bassel-Duby, R., & Olson, E. N. (2012). Control of mitochondrial metabolism and systemic energy homeostasis by MicroRNAs 378 and 378*. *Proceedings of the National Academy of Sciences USA*, *109*, 15330.

Cheng, C. W., Adams, G. B., Perin, L., Wei, M., Zhou, X., Lam, B. S., Sacco, S. Da, Mirisola, M., Quinn, D. I., Dorff, T. B., Kopchick, J. J., & Longo, V. D. (2014). Prolonged fasting reduces IGF-1/PKA to promote hematopoietic-stem-cell- based regeneration and reverse immunosuppression. *Cell Stem Cell*, *14*, 810.

Colman, R. J., Anderson, R. M., Johnson, S. C., Kastman, E. K., Kosmatka, K. J., Beasley, T. M., Allison, D. B., Cruzen, C., Simmons, A., Kemnitz, J. W., & Weindruch, R. (2009). Dietary restriction delays disease onset and mortality in rhesus monkeys. *Science*, *325*, 201.

Czosseck, A., Chen, M. M., Nguyen, H., Meeson, A., Hsu, C., Chen, C., George, T. A., Ruan, S., Cheng, Y., Lin, P., Hsieh, P. C. H., & Lundy, D. J. (2022). Porous scaffold for mesenchymal cell encapsulation and exosome-based therapy of ischemic diseases. *Journal of Controlled Release*, *352*, 879.

de Groot, S., Lugtenberg, R. T., Cohen, D., Welters, M. J. P., Ehsan, I., Vreeswijk, M. P. G., Smit, V. T. H. B. M., de Graaf, H., Heijns, J. B., Portielje, J. E. A., van de Wouw, A. J., Imholz, A. L. T., Kessels, L. W., Vrijaldenhoven, S., Baars, A., Kranenbarg, E. M. K., de Carpentier, M. D., Putter, H., van der Hoeven, J. J. M., …Kroep, J. R. (2020). Fasting mimicking diet as an adjunct to neoadjuvant chemotherapy for breast cancer in the multicentre randomized phase 2 DIRECT trial. *Nature Communications*, *11*, 3083.

Edwards, A. G., Donato, A. J., Lesniewski, L. A., Gioscia, R. A., Seals, D. R., & Moore, R. L. (2010). Life-long caloric restriction elicits pronounced protection of the aged myocardium: A role for AMPK. *Mechanisms of Ageing and Development*, *131*, 739.

Gallet, R., Dawkins, J., Valle, J., Simsolo, E., De Couto, G., Middleton, R., Tseliou, E., Luthringer, D., Kreke, M., Smith, R. R., Marbán, L., Ghaleh, B., & Marbán, E. (2017). Exosomes secreted by cardiosphere-derived cells reduce scarring, attenuate adverse remodelling, and improve function in acute and chronic porcine myocardial infarction. *European Heart Journal*, *38*, 201.

Gangadaran, P., Rajendran, R. L., Lee, H. W., Kalimuthu, S., Hong, C. M., Jeong, S. Y., Lee, S. W., Lee, J., & Ahn, B. C. (2017). Extracellular vesicles from mesenchymal stem cells activates VEGF receptors and accelerates recovery of hindlimb ischemia. *Journal of Controlled Release*, *264*, 112.

Gardner, E. M. (2005). Caloric restriction decreases survival of aged mice in response to primary influenza infection. *Journals of Gerontology - Series A Biological Sciences and Medical Sciences*, *60*, 688.

Ge, X., Meng, Q., Wei, L., Liu, J., Li, M., Liang, X., Lin, F., Zhang, Y., Li, Y., Liu, Z., Fan, H., & Zhou, X. (2021). Myocardial ischemia-reperfusion induced cardiac extracellular vesicles harbour proinflammatory features and aggravate heart injury. *Journal of Extracellular Vesicles*, *10*, e12072.

George, T. A., Hsu, C., Meeson, A., & Lundy, D. J. (2022). Nanocarrier-based targeted therapies for myocardial infarction. *Pharmaceutics*, *14*, 930.

Gerczuk, P. Z., & Kloner, R. A. (2012). An update on cardioprotection: A review of the latest adjunctive therapies to limit myocardial infarction size in clinical trials. *Journal of the American College of Cardiology*, *59*, 969.

Grundmann, F., Müller, R. U., Reppenhorst, A., Hülswitt, L., Späth, M. R., Kubacki, T., Scherner, M., Faust, M., Becker, I., Wahlers, T., Schermer, B., Benzing, T., & Burst, V. (2018). Preoperative short-term calorie restriction for prevention of acute kidney injury after cardiac surgery: A randomized, controlled, open-label, pilot trial. *Journal of the American Heart Association*, *7*, e008181.

Harvey, A. E., Lashinger, L. M., Hays, D., Harrison, L. M., Lewis, K., Fischer, S. M., & Hursting, S. D. (2014). Calorie restriction decreases murine and human pancreatic tumor cell growth, nuclear factor-ĸB activation, and inflammation-related gene expression in an insulin-like growth factor-1 - dependent manner. *PLoS One*, *9*, 1.

Helwa, I., Cai, J., Drewry, M. D., Zimmerman, A., Dinkins, M. B., Khaled, M. L., Seremwe, M., Dismuke, W. M., Bieberich, E., Stamer, W. D., Hamrick, M. W., & Liu, Y. (2017). A comparative study of serum exosome isolation using differential ultracentrifugation and three commercial reagents. *PLoS One*, *12*, 1.

Horowitz, A. M., Fan, X., Bieri, G., Smith, L. K., Sanchez-Diaz, C. I., Schroer, A. B., Gontier, G., Casaletto, K. B., Kramer, J. H., Williams, K. E., & Villeda, S. A. (2020). Blood factors transfer beneficial effects of exercise on neurogenesis and cognition to the aged brain. *Science*, *369*, 167.

Huang, X., Yuan, T., Tschannen, M., Sun, Z., Jacob, H., Du, M., Liang, M., Dittmar, R. L., Liu, Y., Liang, M., Kohli, M., Thibodeau, S. N., Boardman, L., & Wang, L. (2013). Characterization of human plasma-derived exosomal RNAs by deep sequencing. *BMC Genomics*, *14*, 1.

Ingram, D. K., & de Cabo, R. (2017). Calorie restriction in rodents: Caveats to consider. *Ageing Research Reviews*, *39*, 15.

Kristan, D. M. (2007). Chronic calorie restriction increases susceptibility of laboratory mice (Mus Musculus) to a primary intestinal parasite infection. *Aging Cell*, *6*, 817.

Kugeratski, F. G., Hodge, K., Lilla, S., McAndrews, K. M., Zhou, X., Hwang, R. F., Zanivan, S., & Kalluri, R. (2021). Quantitative proteomics identifies the core proteome of exosomes with syntenin-1 as the highest abundant protein and a putative universal biomarker. *Nature Cell Biology*, *23*, 631.

Lai, J. J., Chau, Z. L., Chen, S. Y., Hill, J. J., Korpany, K. v., Liang, N. W., Lin, L. H., Lin, Y. H., Liu, J. K., Liu, Y. C., Lunde, R., & Shen, W. T. (2022). Exosome processing and characterization approaches for research and technology development. *Advanced Science*, *1*, 2103222.

Lee, E. K., Jeong, H. O., Bang, E. J., Kim, C. H., Mun, J. Y., Noh, S., Gim, J. A., Kim, D. H., Chung, K. W., Yu, B. P., & Chung, H. Y. (2018). The involvement of serum exosomal MiR-500-3p and MiR-770- 3p in aging: Modulation by calorie restriction. *Oncotarget*, *9*, 5578.

Liu, C., Min, L., Kuang, J., Zhu, C., Qiu, X. Y., & Zhu, L. (2019). Bioinformatic identification of MiR-622 key target genes and experimental validation of the MiR-622-RNF8 axis in breast cancer. *Frontiers in Oncology*, *9*, 1114.

Liu, J. R., Cai, G. Y., Ning, Y. C., Wang, J. C., Lv, Y., Guo, Y. N., Fu, B., Hong, Q., Sun, X. F., & Chen, X. M. (2020). Caloric restriction alleviates aging-related fibrosis of kidney through downregulation of MiR-21 in extracellular vesicles. *Aging*, *12*, 18052.

Lu, Y. A., Te Liao, C., Raybould, R., Talabani, B., Grigorieva, I., Szomolay, B., Bowen, T., Andrews, R., Taylor, P. R., & Fraser, D. (2021). Single-nucleus RNA sequencing identifies new classes of proximal tubular epithelial cells in kidney fibrosis. *Journal of the American Society of Nephrology*, *32*, 2501.

Luo, Z., Hu, X., Wu, C., Chan, J., Liu, Z., Guo, C., Zhu, R., Zhang, L., Zhang, Y., Jin, S., & He, S. (2023). Plasma exosomes generated by ischaemic preconditioning are cardioprotective in a rat heart failure model. *British Journal of Anaesthesia*, *130*, 29.

Mahoney, L. B., Denny, C. A., & Seyfried, T. N. (2006). Caloric restriction in C57BL/6J mice mimics therapeutic fasting in humans. *Lipids in Health and Disease*, *5*, 1.

Mitchell, J. R., Verweij, M., Brand, K., van de Ven, M., Goemaere, N., van den Engel, S., Chu, T., Forrer, F., Müller, C., de Jong, M., van IJcken, W., IJzermans, J. N. M., Hoeijmakers, J. H. J., & de Bruin, R. W. F. (2010). Short-term dietary restriction and fasting precondition against ischemia reperfusion injury in mice. *Aging Cell*, *9*, 40.

Mitchell, S. J., Bernier, M., Mattison, J. A., Aon, M. A., Kaiser, T. A., Anson, R. M., Ikeno, Y., Anderson, R. M., Ingram, D. K., & de Cabo, R. (2019). Daily Fasting improves health and survival in male mice independent of diet composition and calories. *Cell Metabolism*, *29*, 221.

Most, J., Tosti, V., Redman, L. M., & Fontana, L. (2017). Calorie restriction in humans: An update. *Ageing Research Reviews*, *39*, 36.

Murray, P. J., Allen, J. E., Biswas, S. K., Fisher, E. A., Gilroy, D. W., Goerdt, S., Gordon, S., Hamilton, J. A., Ivashkiv, L. B., Lawrence, T., Locati, M., Mantovani, A., Martinez, F. O., Mege, J. L., Mosser, D. M., Natoli, G., Saeij, J. P., Schultze, J. L., Shirey, K. A., …Wynn, T. A. (2014). Macrophage activation and polarization: Nomenclature and experimental guidelines. *Immunity*, *41*, 14.

Nencioni, A., Caffa, I., Cortellino, S., & Longo, V. D. (2018). Fasting and cancer: Molecular mechanisms and clinical application. *Nature Reviews Cancer*, *18*, 707.

Newman, J. C., & Verdin, E. (2014). Ketone bodies as signaling metabolites. *Trends in Endocrinology & Metabolism*, *25*, 42.

Ning, Y. C., Cai, G. Y., Zhuo, L., Gao, J. J., Dong, D., Cui, S. Y., Shi, S. Z., Feng, Z., Zhang, L., Sun, X. F., & Chen, X. M. (2014). Beneficial effects of short-term calorie restriction against cisplatin-induced acute renal injury in aged rats. *Nephron Experimental Nephrology*, *124*, 19.

Ojha, N., Roy, S., Radtke, J., Simonetti, O., Gnyawali, S., Zweier, J. L., Kuppusamy, P., & Sen, C. K. (2008). Characterization of the structural and functional changes in the myocardium following focal ischemia-reperfusion injury. *American Journal of Physiology - Heart and Circulatory Physiology*, *294*, H2435.

Osorio-Querejeta, I., Carregal-Romero, S., Ayerdi-Izquierdo, A., Mäger, I., Nash, L. A., Wood, M., Egimendia, A., Betanzos, M., Alberro, A., Iparraguirre, L., Moles, L., Llarena, I., Möller, M., Goñi-De-cerio, F., Bijelic, G., Ramos-Cabrer, P., Muñoz-Culla, M., & Otaegui, D. (2020). MiR-219a-5p enriched extracellular vesicles induce OPC differentiation and EAE improvement more efficiently than liposomes and polymeric nanoparticles. *Pharmaceutics*, *12*, 186.

Prasad, A., Stone, G. W., Holmes, D. R., & Gersh, B. (2009). Reperfusion injury, microvascular dysfunction, and cardioprotection: The "Dark Side" of reperfusion. *Circulation*, *120*, 2105.

Ritz, B. W., Nogusa, S., & Gardner, E. M. (2007). Caloric restriction increases early susceptibility to influenza infection in young C57BL/6 mice despite an intact NK cell response. *The FASEB Journal*, *21*, A47–A47.

Scarabelli, T., Stephanou, A., Rayment, N., Pasini, E., Comini, L., Curello, S., Ferrari, R., Knight, R., & Latchman, D. (2001). Apoptosis of endothelial cells precedes myocyte cell apoptosis in ischemia/reperfusion injury. *Circulation*, *104*, 253.

Shah, R., Patel, T., & Freedman, J. E. (2018). Circulating extracellular vesicles in human disease. *New England Journal of Medicine*, *379*, 958.

Sharfuddin, A. A., & Molitoris, B. A. (2011). Pathophysiology of ischemic acute kidney injury. *Nature Reviews Nephrology*, *7*, 189.

Shi, H., Zhang, X., He, Z., Wu, Z., Li, Y., & Rao, L. (2017). Metabolites of hypoxic cardiomyocytes induce the migration of cardiac fibroblasts. *Cellular Physiology and Biochemistry*, *41*, 413.

Shin, N. S., Marlier, A., Xu, L., Doilicho, N., Linberg, D., Guo, J., & Cantley, L. G. (2022). Arginase-1 is required for macrophage-mediated renal tubule regeneration. *Journal of the American Society of Nephrology*, *33*, 1077.

Soler-Botija, C., Monguió-Tortajada, M., Munizaga-Larroudé, M., Gálvez-Montón, C., Bayes-Genis, A., & Roura, S. (2022). Mechanisms governing the therapeutic effect of mesenchymal stromal cell-derived extracellular vesicles: A scoping review of preclinical evidence. *Biomedicine and Pharmacotherapy*, *147*, 112683.

Sun, D., Muthukumar, A. R., Lawrence, R. A., & Fernandes, G. (2001). Effects of calorie restriction on polymicrobial peritonitis induced by cecum ligation and puncture in young C57BL/6 mice. *Clinical and Diagnostic Laboratory Immunology*, *8*, 1003.

Théry, C., Witwer, K. W., Aikawa, E., Alcaraz, M. J., Anderson, J. D., Andriantsitohaina, R., Antoniou, A., Arab, T., Archer, F., Atkin-Smith, G. K., Ayre, D. C., Bach, J. M., Bachurski, D., Baharvand, H., Balaj, L., Baldacchino, S., Bauer, N. N., Baxter, A. A., Bebawy, M., …Zuba-Surma, E. K. (2018). Minimal information for studies of extracellular vesicles 2018 (MISEV2018): A position statement of the international society for extracellular vesicles and update of the MISEV2014 guidelines. *Journal of Extracellular Vesicles*, *7*, 1535750.

Vanderboom, P. M., Dasari, S., Ruegsegger, G. N., Pataky, M. W., Lucien, F., Heppelmann, C. J., Lanza, I. R., & Nair, K. S. (2021). A size-exclusion-based approach for purifying extracellular vesicles from human plasma. *Cell Reports Methods*, *1*, 100055.

Vega, V. L., de Cabo, R., & De Maio, A. (2004). Age and caloric restriction diets are confounding factors that modify the response to lipopolysaccharide by peritoneal macrophages in C57BL/6 mice. *Shock*, *22*, 248.

Vicencio, J. M., Yellon, D. M., Sivaraman, V., Das, D., Boi-Doku, C., Arjun, S., Zheng, Y., Riquelme, J. A., Kearney, J., Sharma, V., Multhoff, G., Hall, A. R., & Davidson, S. M. (2015). Plasma exosomes protect the myocardium from ischemia-reperfusion injury. *Journal of the American College of Cardiology*, *65*, 1525.

Wang, C., Li, L., Yang, C., Zhang, Z., Li, X., Wang, Y., Lv, X., Qi, X., & Song, G. (2022). One night of sleep deprivation induces release of small extracellular vesicles into circulation and promotes platelet activation by small EVs. *Journal of Cellular and Molecular Medicine*, *1*, 5033–5043.

Wang, J., Tan, J., Qi, Q., Yang, L., Wang, Y., Zhang, C., Hu, L., Chen, H., & Fang, X. (2018). MiR-487b-3p suppresses the proliferation and differentiation of myoblasts by targeting IRS1 in skeletal muscle myogenesis. *International Journal of Biological Sciences*, *14*, 760.

Wei, M., Brandhorst, S., Shelehchi, M., Mirzaei, H., Cheng, C. W., Budniak, J., Groshen, S., Mack, W. J., Guen, E., Di Biase, S., Cohen, P., Morgan, T. E., Dorff, T., Hong, K., Michalsen, A., Laviano, A., & Longo, V. D. (2017). Fasting-mimicking diet and markers/risk factors for aging, diabetes, cancer, and cardiovascular disease. *Science Translational Medicine*, *9*, eaai8700.

Widyaningrum, R., Burnouf, T., Nebie, O., Delila, L., & Wang, T. J. (2021). A purified human platelet pellet lysate rich in neurotrophic factors and antioxidants repairs and protects corneal endothelial cells from oxidative stress. *Biomedicine and Pharmacotherapy*, *142*, 112046.

Willms, E., Johansson, H. J., Mäger, I., Lee, Y., Blomberg, K. E. M., Sadik, M., Alaarg, A., Smith, C. I. E., Lehtiö, J., El Andaloussi, S., Wood, M. J. A., & Vader, P. (2016). Cells release subpopulations of exosomes with distinct molecular and biological properties. *Scientific Reports*, *6*, 1.

Witwer, K. W., Buzás, E. I., Bemis, L. T., Bora, A., Lässer, C., Lötvall, J., Nolte-'t Hoen, E. N., Piper, M. G., Sivaraman, S., Skog, J., Théry, C., Wauben, M. H., & Hochberg, F. (2013). Standardization of sample collection, isolation and analysis methods in extracellular vesicle Research. *Journal of Extracellular Vesicles*, *2*, 20360.

World Health Organization. The top 10 causes of death. https://www.who.int/news-room/fact-sheets/detail/the-top-10-causes-of-death

Xiang, Y., Eyers, F., Herbert, C., Tay, H. L., Foster, P. S., & Yang, M. (2016). MicroRNA-487b is a negative regulator of macrophage activation by targeting IL-33 production. *The Journal of Immunology*, *196*, 3421.

Youm, Y. H., Nguyen, K. Y., Grant, R. W., Goldberg, E. L., Bodogai, M., Kim, D., D'Agostino, D., Planavsky, N., Lupfer, C., Kanneganti, T. D., Kang, S., Horvath, T. L., Fahmy, T. M., Crawford, P. A., Biragyn, A., Alnemri, E., & Dixit, V. D. (2015). The Ketone Metabolite β-Hydroxybutyrate Blocks NLRP3 Inflammasome-Mediated Inflammatory Disease. *Nature Medicine*, *21*, 263.

Zhao, H., Chen, X., Hu, G., Li, C., Guo, L., Zhang, L., Sun, F., Xia, Y., Yan, W., Cui, Z., Guo, Y., Guo, X., Huang, C., Fan, M., Wang, S., Zhang, F., & Tao, L. (2022). Small extracellular vesicles from brown adipose tissue mediate exercise cardioprotection. *Circulation Research*, *130*, 1490.

SUPPORTING INFORMATION

Additional supporting information can be found online in the Supporting Information section at the end of this article.